

## LATITUDINAL STRUCTURE OF THE NIGHTSIDE REGION 1 FIELD-ALIGNED CURRENT OBSERVED FROM THE EXOS-D SATELLITE

Takashi YAMAMOTO<sup>1</sup>, Shoshi INOUE<sup>2</sup> and Masao OZAKI<sup>3</sup>

<sup>1</sup> *Department of Earth and Planetary Physics, University of Tokyo, Hongo  
7-chome, Bunkyo-ku, Tokyo 113-0033*

<sup>2</sup> *Aichi College of Technology, Manori, Nishihazama-cho, Gamagori 443-0047*

<sup>3</sup> *Institute of Industrial Science, University of Tokyo, Roppongi  
7-chome, Minato-ku, Tokyo 106-8558*

**Abstract:** The average pattern of region 1 field-aligned current (FAC) of IJIMA and POTEMRA (J. Geophys. Res., **81**, 2165, 1976a; J. Geophys. Res., **83**, 599, 1978) spans 2–3° in magnetic latitude. Using the magnetic field data acquired with the EXOS-D satellite, we notice that sharp variations of magnetic field perturbation, showing the high current densities of several micro-amperes per squared meter at the ionospheric height, are included in the region 1 current zone. In this paper, we focus our analysis on a sharp gradient of magnetic field change within 1° in latitude. In the 20–04 MLT sector, the thin current sheet as an important part of the region 1 FAC system is often found to be just equatorward of the boundary FAC system (FUKUNISHI *et al.*, J. Geophys. Res., **98**, 11235, 1993). A statistical survey of more than 200 satellite's crossings of the region 1 zone (in the 17–05 MLT range) shows that about 60% of the identified region 1 current systems have the latitudinal structure of a thin (on average, 0.5°) current sheet with current intensity greater than one third of the total FAC intensity of the region 1 system.

### 1. Introduction

The field-aligned currents (FACs) flowing between the magnetosphere and the polar ionosphere have been investigated by the magnetometer and charged particle measurements from satellites and rockets. Using the magnetometer data from the TRIAD satellite, IJIMA and POTEMRA (1976a, b, 1978) have shown the statistical characteristics of the large-scale FACs, identifying three principal regions of FACs, namely the region 1, region 2 and the cusp region. Over the high-latitude part of the aurora oval, the region 1 currents flow into (downward) the ionosphere on the morningside and away from (upward) the ionosphere on the eveningside. Over the low-latitude part of the aurora oval, the region 2 currents flow upward and downward on the morningside and eveningside, respectively. Later, using the high time-resolution magnetometer data from the Dynamic Explorer 1 (DE-1), Dynamic Explorer 2 (DE-2) and Viking satellites, the small-scale (<0.5° in latitude) FACs have been identified by, *e.g.*, CRAVEN *et al.* (1983), POTEMRA *et al.* (1987) and BYTHROW *et al.* (1987). Basically, the observations from satellites at relatively high (say, ~10000 km) altitudes, such as

the DE-1 and Viking, have the advantage of more easily identifying the fine structure of the FACs because the Earth field lines diverge with the distance from the ground and the speed of a satellite is slower at higher altitudes. The high time-resolution data can also be provided by the EXOS-D satellite which was launched on February 21, 1989, into a polar elliptical orbit with apogee of 10500 km, perigee of 274 km and inclination of  $75.0^\circ$ . Analyzing the EXOS-D magnetometer data, FUKUNISHI *et al.* (1991) have shown that small-scale FACs with latitudinal width of  $0.05^\circ$ – $0.2^\circ$  always exist in the large-scale region 1, region 2, cusp and polar cap current systems. Furthermore, it has been shown that the boundary FAC system, namely the paired downward and upward FACs almost always exist along the poleward boundary of the nightside auroral oval (FUKUNISHI *et al.*, 1993; NAGATSUMA *et al.*, 1995). Such a current system has also been discussed by FUJII *et al.* (1994), on the basis of the DE-1 and DE-2 observations. (More recently, the particle and magnetic field data with high temporal/spatial resolution have been acquired with the low-altitude satellite Freja. This satellite mission was designed to investigate small-scale auroral phenomena (*e.g.*, HAERENDEL *et al.*, 1994). Small-scale FACs with thickness down even to a few hundred meters have been studied by STASIEWICZ and POTEMRA (1998) and YAMAUCHI *et al.* (1998).)

In the present paper we study the latitudinal structure of the nightside region 1 FACs, using the magnetic field data from the EXOS-D in the period from 1 August 1989 to 12 September 1990, during which the satellite traversed the nightside auroral oval at altitudes of 4000–10000 km. We are particularly interested in the case that the nearly entire region 1 currents are concentrated to a narrow region of latitudinal width of  $\sim 0.5^\circ$ . In such a case there is no distinction between the so-called small-scale and large-scale FACs. Notably, this fact is in contrast with the previous supposition that small-scale FACs are embedded in the large-scale region 1 FAC system. Hence, in the next section we propose a new definition of the global and local FAC systems, based on the spatial scales over which the corresponding charge separation processes occur in the magnetosphere. In Section 3, we present the preliminary results of statistical investigation on the latitudinal concentration of nightside region 1 currents, although the number of data analyzed so far is limited.

## 2. Local and Global FAC Systems

According to YAMAMOTO *et al.* (1997a,b), the quasi-steady FACs can be given birth to by the action of magnetic drifts of plasma particles when the distribution of the flux tube content,  $N$ , of the hot (1–10 keV) particles is nonuniform and distorted by the plasma convection. (The distorted  $N$  means that the equiconours of  $N$  (on the ionospheric plane) are not parallel to the direction of the average magnetic drift velocity projected to the ionosphere. In terms of the flux tube content, a number of authors (*e.g.*, VASYLIUNAS (1970); SOUTHWOOD (1977); HAREL *et al.* (1981); WOLF (1983); HEINEMANN *et al.* (1989); YANG *et al.* (1994)) have discussed the generation of FACs in the auroal zone. For a review, see YAMAMOTO *et al.* (1996).) The FACs can also be produced by an anomalous cross-field diffusion of ions when  $N$  is nonuniform. By assuming, in the nighttime auroral oval, the distorted plasma distribution with azimuthally-aligned striations, we can conceptually understand the generations of

various current systems such as the region 1 and region 2 FACs, the triple FACs in the midnight sector, the boundary FACs (FUKUNISHI *et al.*, 1993) and the (coupled or triple) FACs of narrow widths which are associated with discrete auroras. For some of these FAC systems, Fig. 1 schematically illustrates how the corresponding charge separations might occur in the magnetosphere. (In this figure, the charge separation processes are projected to the ionosphere.) For detailed discussion, see YAMAMOTO *et al.* (1997a, b). (Recently, a distorted  $N$  profile of hot particles is produced in numerical simulations by YAMAMOTO and INOUE (1998), under the condition that particle energization (e.g., LYONS and SPEISER, 1982) takes place just inside the open/close boundary which is assumed to be subject to convection distortion. This condition is likely to be satisfied in periods of southward interplanetary magnetic field (IMF). In fact, YAMAMOTO *et al.* (1999) have shown that distortion of the outer boundary of the closed region occurs in the Tsyganenko magnetic field model (TSYGANENKO, 1989) in case of southward IMF.)

Specifically, for two simple latitudinal  $N$ -profiles of the source plasma as schematically shown in the first column of Fig. 2, we discuss the FACs produced by the above two mechanisms. The profiles of FAC density ( $J_{\parallel}$ ) and associated magnetic

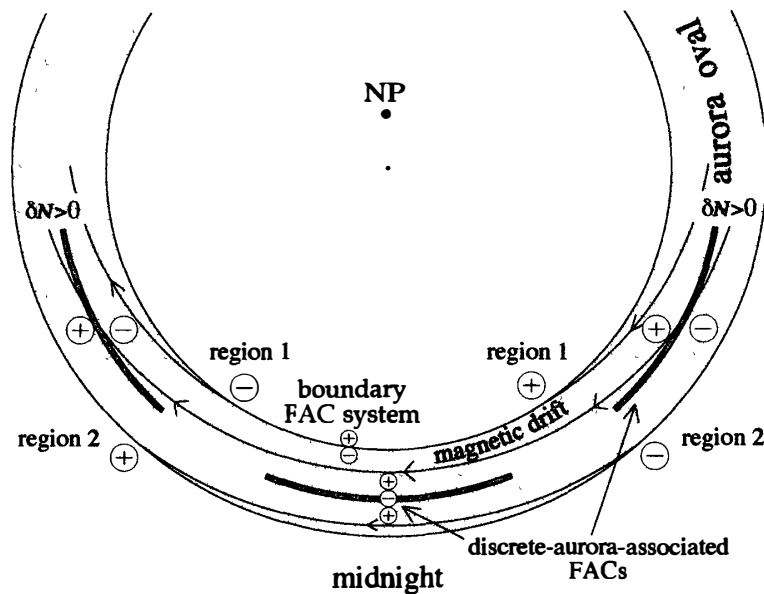


Fig. 1. Schematic illustration of various processes of charge separation in the auroral magnetosphere, which are projected to the ionosphere. The production of positive or negative charges (designated by symbol + or -) induces field-aligned currents flowing into or away from the ionosphere, respectively. In the FAC model by YAMAMOTO *et al.* (1997a, b), the region 1 and region 2 currents are assumed to be created, by the action of magnetic drift, on the distorted distribution of the flux tube content  $N$  of the hot (1-10 keV) plasma particles, during the period of southward interplanetary magnetic field. The anomalous cross-field diffusion of ions can lead to the generation of the triple FACs in the midnight-sector, the boundary FACs, and the discrete-aurora-associated FACs (if small-scale striations in  $N$  are produced).

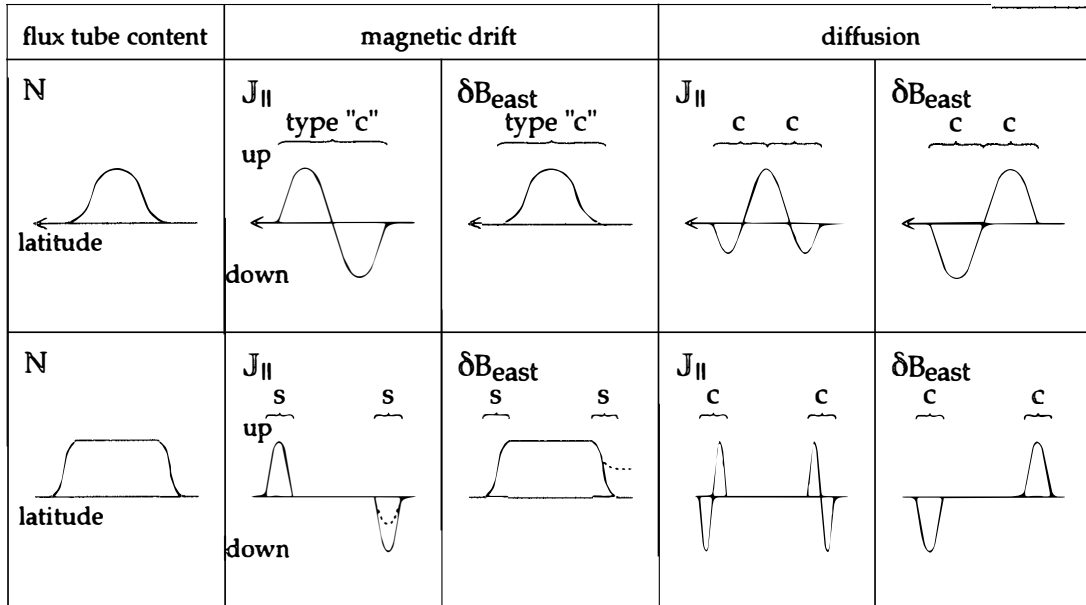


Fig. 2. Schematic illustration of latitudinal profiles of FAC densities ( $J_{\parallel}$ ) and associated magnetic disturbances ( $\delta B_{\text{east}}$ ), produced on the auroral particle distributions with profiles of flux tube content ( $N$ ) indicated in the respective rows, the first column, by the actions of particle magnetic drift and ion cross-field diffusion. (For more explanation, see text.)

disturbance (longitudinal component,  $\delta B_{\text{east}}$ ), produced on respective  $N$ -profiles by respective mechanisms, are schematically shown in Fig. 2. Here the two mechanisms for FAC generation are simply designated as ‘magnetic drift’ and ‘diffusion’, and the FACs by magnetic drift are illustrated as those on the eveningside auroral oval with convection distortion (YAMAMOTO *et al.*, 1997a); the disturbance  $\delta B_{\text{east}}$  is assumed to be estimated under the current-sheet approximation that the FACs are represented by current-sheets of infinite extent. In the bottom row of this figure, FACs appear near the both edges of the source plasma ( $N > 0$ ). In this case it is assumed that the FACs near the each edge belong to one FAC system so that two separate FAC systems are formed. All the FAC systems depicted in Fig. 2 are referred to as the “elementary FAC systems”, implying that the actual FACs are presumed to consist of these elementary systems. The  $J_{\parallel}$ -profiles in individual elementary FAC systems are simply classified into two types: one is a couple of upward and downward currents, and the other is an isolated upward or downward current. In Fig. 2, the former and latter types are labelled “c” and “s”, respectively (where “c” and “s” mean “couple” and “single”, respectively). Correspondingly, the  $\delta B_{\text{east}}$ -profiles are classified into two types of “c” and “s”: type c is in the form of a simple peak or trough, and type s is in the form of a step.

Now, for the elementary FAC systems we make a distinction between the local and global ones, in terms of the latitudinal change in the magnetic disturbance ( $\delta B_{\text{east}}$ ). The local FAC system is defined as the one causing  $\delta B_{\text{east}}$  satisfying the conditions that the region of  $d(\delta B_{\text{east}})/d\theta \neq 0$  ( $\theta$  is the latitude) is confined to a latitudinal interval of less than about  $2^{\circ}$  and its net change over this interval is even smaller than the maximum amplitude of  $\delta B_{\text{east}}$ . Needless to say, the both conditions mean that the total width of

the elementary FAC system is less than about  $2^\circ$  and the upward and downward FACs in the system are almost equal in intensity. (Note that in practice it is necessary to define the local/global FAC systems in terms of the magnetic disturbance because we can usually identify the FACs by observing the magnetic disturbances.) Any elementary FAC system other than the local one is referred to as the global elementary FAC system. The FAC system with substantial net change of  $\delta B_{\text{east}}$  across it (see type s in the bottom row of Fig. 2) is defined to be global, however narrow its latitudinal width may be. The global FAC system with a narrow width of  $\leq 0.5^\circ$  can sometimes be identified from the EXOS-D MGF data. (Such an example will be shown below.) Notably, the above classification of the local and global FAC systems are implicitly based on the spatial dimension of a region where the corresponding charge separation takes place.

As is noted above, the actual FACs consist of the local and global elementary systems; in the nighttime auroral oval, the typical local elementary systems are the boundary FAC system and the discrete-aurora-associated coupled and triple FACs, and the global ones are the region 1 and region 2 FACs and the midnight triple FACs. Keeping this fact in view, here we make an attempt to decompose the observed  $\delta B_{\text{east}}$  into elementary components, each of which is pertinent to the signature of one elementary FAC system (although unambiguous decomposition is sometimes difficult). Such an

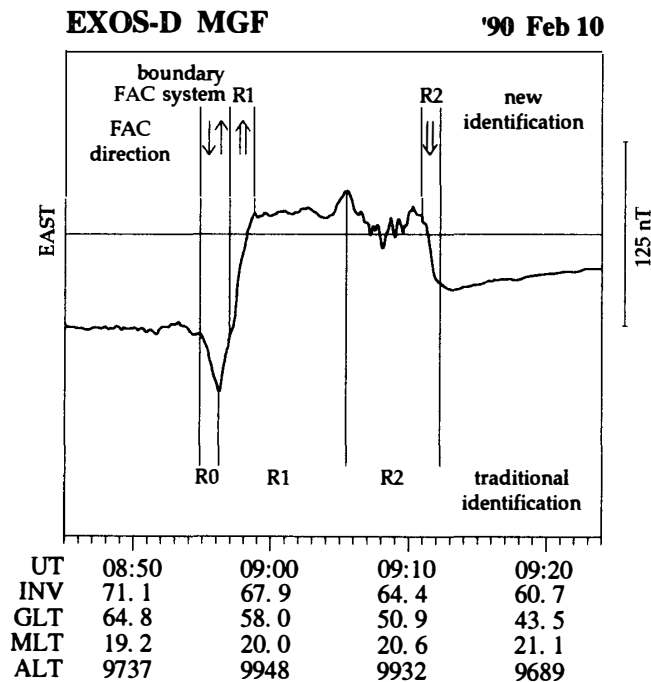


Fig. 3. East-west component of magnetic field perturbation obtained from the EXOS-D observations on February 10, 1990. According to our definitions of the local and global FACs (see text), the regions of the boundary FAC system, the region 1 FAC and the region 2 FAC are indicated above the curve of magnetic perturbation. (The boundary FAC system may partly overlap with the region 1 system. In this figure, for simplicity, we assume that there is a single interface between them.) Below the magnetic perturbation curve, illustrated is the traditional identification of the region 0, region 1 and region 2 FAC zones.

example is shown in Fig. 3, where the traditional division into the region 0, region 1 and region 2 zones is also indicated (see, *e.g.*, POTEMRA *et al.*, 1987). In our identification, each FAC signature between the region 1 and the region 2 FACs is assumed to belong to one of several local current systems there. Notably, the upward FAC which is labelled “R1” according to our definition brings about a significant increase ( $\sim 80$  nT) of  $\delta B_{\text{east}}$  in a narrow interval of about  $0.5^\circ$ . According to the traditional classification, this part (as well as the upward current just poleward of it) must be identified as a small-scale current imbedded in the large-scale region 1 current. It is physically natural that the FAC with a significant change of  $\delta B_{\text{east}}$  (implying a significant contribution to the polar cap potential drop) is regarded as a global FAC system. Moreover, note that in the magnetosphere, such a (region 1) FAC system might be connected to its counterpart (region 1) by a long (virtual) path of the charge separation (see Fig. 1 in this paper as well as Figs. 7 and 8 in YAMAMOTO *et al.* (1997a)), even if either FAC system is confined to a narrow latitude zone. In passing, it is worthy of noting that investigation of the latitudinal structure of a FAC system may be useful for identifying the corresponding charge separation in the magnetosphere and for inferring the distribution of the flux tube content of auroral particles.

### 3. Concentration of Region 1 Current

Figures 4–6 show various types of the (inner) latitudinal structure of the region 1 FAC system, which are identified from the EXOS-D MGF data. (We do not discuss the structure of the region 2 FAC system.) From top to bottom, in each figure, the geomagnetic east-west ( $\delta B_{\text{east}}$ ) and north-south ( $\delta B_{\text{north}}$ ) components of magnetic field, and FAC density (positive values for upward current) are shown. (For detailed explanation of the data, see FUKUNISHI *et al.* (1991, 1993).) In Fig. 4a, the region 1 (upward) FAC system is assumed to consist of the thin and broad (in latitude) structures, which are labelled “T” and “B”, respectively. (As a working hypothesis, we are to identify at most one T-structure and one B-structure in a single region 1 system.) The T-structure is characterized by the narrow latitudinal width of about one degree or less and the relatively high current density. On the other hand, the B-structure is characterized by the width greater than one degree and the low current density. In case of Fig. 4a, on average, the FAC density is  $\sim 0.3 \mu\text{A}/\text{m}^2$  (at the satellite altitude) in the T-structure, and it is  $\sim 0.1 \mu\text{A}/\text{m}^2$  in the B-structure. In general, however, we do not assume any specific value of the average current density as a qualifying condition for the T- or B-structure. Practically, the T-structure is identified when it satisfies the above condition of the scale length and it has an average gradient of  $\delta B_{\text{east}}$  greater, by at least a factor of two, than that averaged over the remaining part of the region 1 system. For a particular case that the total width of the region 1 system is less than one degree, the entire system may be regarded as one T-structure. Such an example is already shown in Fig. 3. To avoid ambiguous identification of the T-structure, we disregard such a minor one as having the current intensity less than one third of the total current intensity of the region 1 system. (Note that the current intensity is proportional to the net change of  $\delta B_{\text{east}}$ .) Namely, in this case the entire region 1 system is assumed to be constituted by the B-structure only. Such a current system is referred to as the

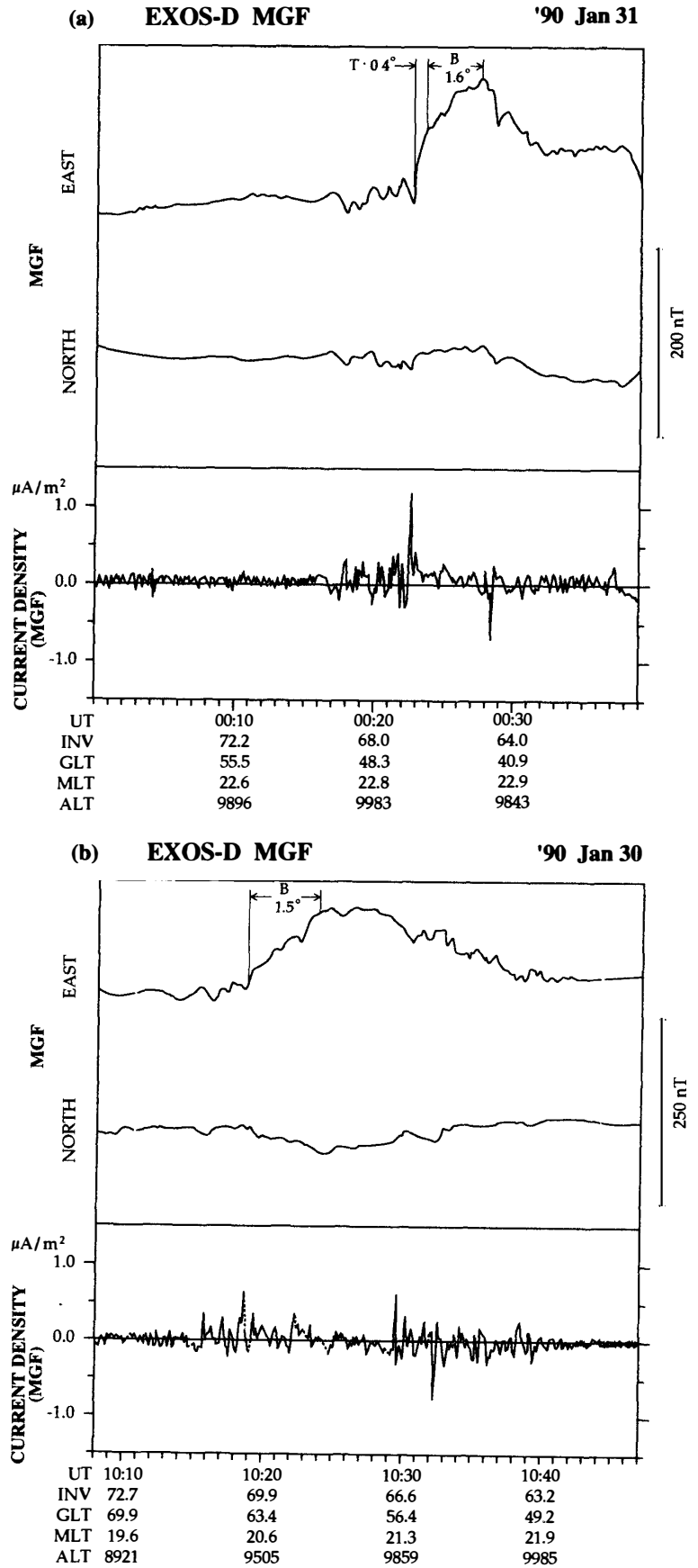
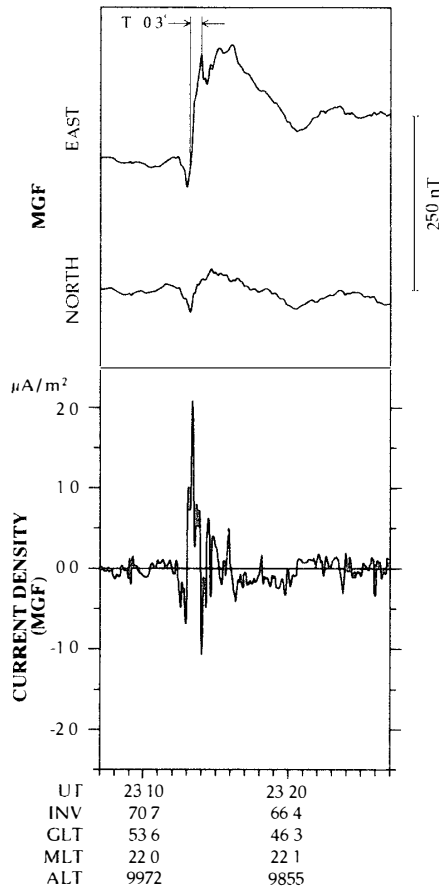


Fig. 4. East-west and north-south components of magnetic field perturbation and field-aligned current density (positive values for upward current) obtained from the EXOS-D observations on (a) January 31, 1990 and (b) January 30, 1990. The T- and B-structures (see text) in each region 1 FAC system are indicated together with their latitudinal widths.

(a) EXOS-D MGF '90 Feb 7



(b) EXOS-D MGF '89 Aug 3

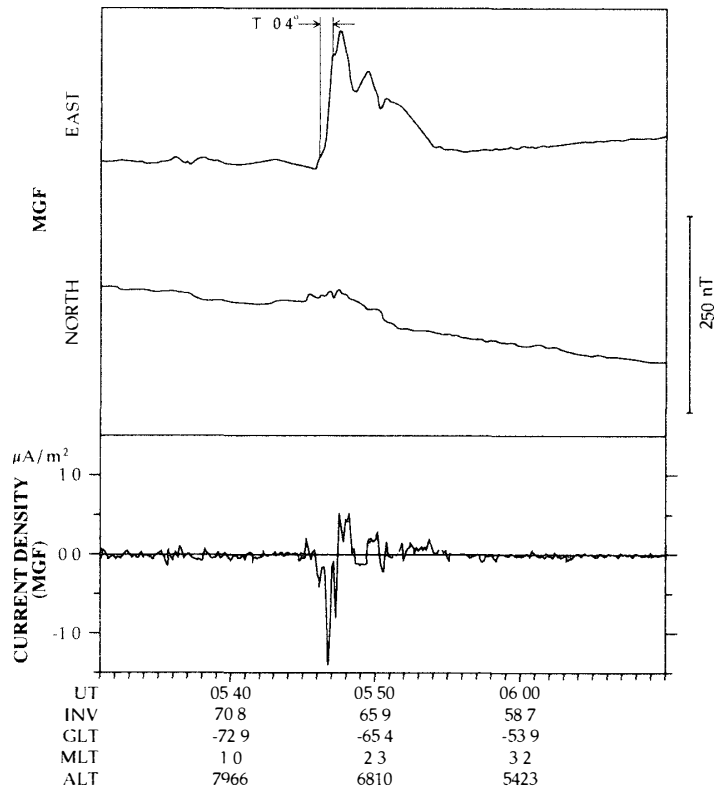


Fig. 5. Same as Fig. 4, but for (a) February 7, 1990 and (b) August 3, 1989.

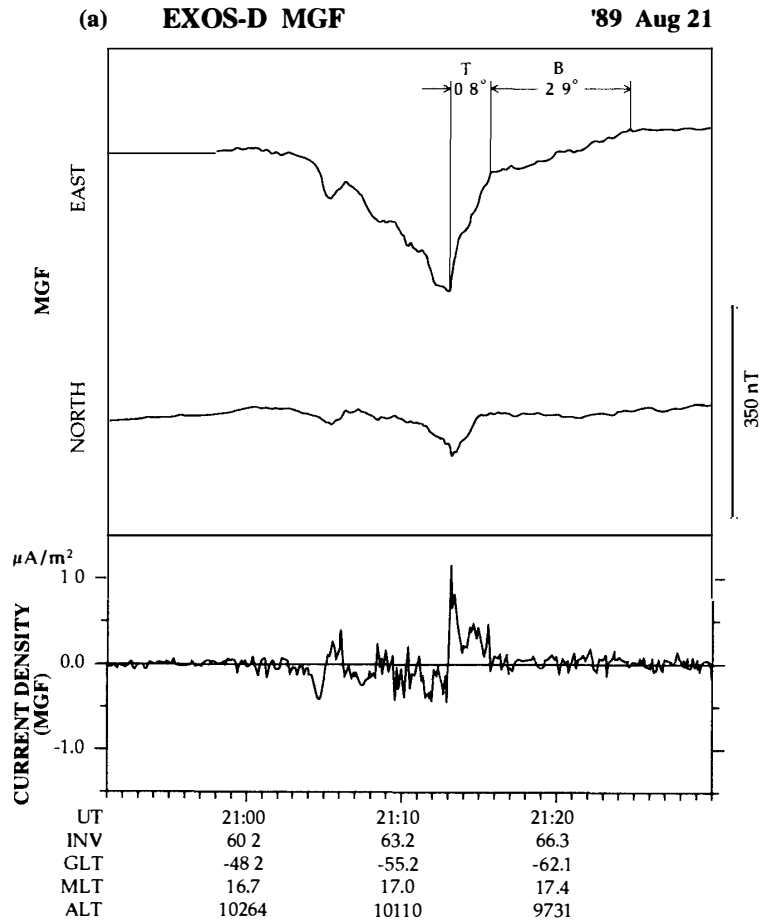


Fig. 6. Same as Fig. 4, but for (a) August 21, 1989 and (b) March 29, 1990.

broad-type region 1 system, and its example is shown in Fig. 4b.

In contrast with the FAC structures in Figs. 4a and 4b, Figs. 5a and 5b (as well as Fig. 3) show examples of the region 1 current system which is essentially formed only by one T-structure. In the 20–04 MLT sector, when the T-structure is identified, it almost always constitutes the most poleward portion of a single region 1 current system. More specifically, if the boundary FAC system (FUKUNISHI *et al.*, 1993) is identified too, the T-structure is located just equatorward of the boundary FAC system while they may partly overlap each other. In the dusk (~18 MLT) or the dawn (~06 MLT) sector, when the T-structure is identified, it tends to constitute the highest or lowest latitude portion of a single region 1 system. Examples of the latter configurations in the dusk and dawn sectors are shown in Figs. 6a and 6b, respectively. (More closely looking into the current density profiles in Figs. 4–6, we may suppose that the T-structure consists of thinner and denser current-sheets. Such fine structures of FACs have recently been studied by STASIEWICZ and POTEMRA (1998) and YAMAUCHI *et al.* (1998) with the Freja data.)

Finally, we present the results of statistical investigation to see how often the T-structure appears in the nightside region 1 FAC system. In Fig. 7a, the numbers of region 1 current systems identified in the present analysis is plotted against the (total) latitudinal width. Also, the gray-shaded part of the histogram indicates the numbers of

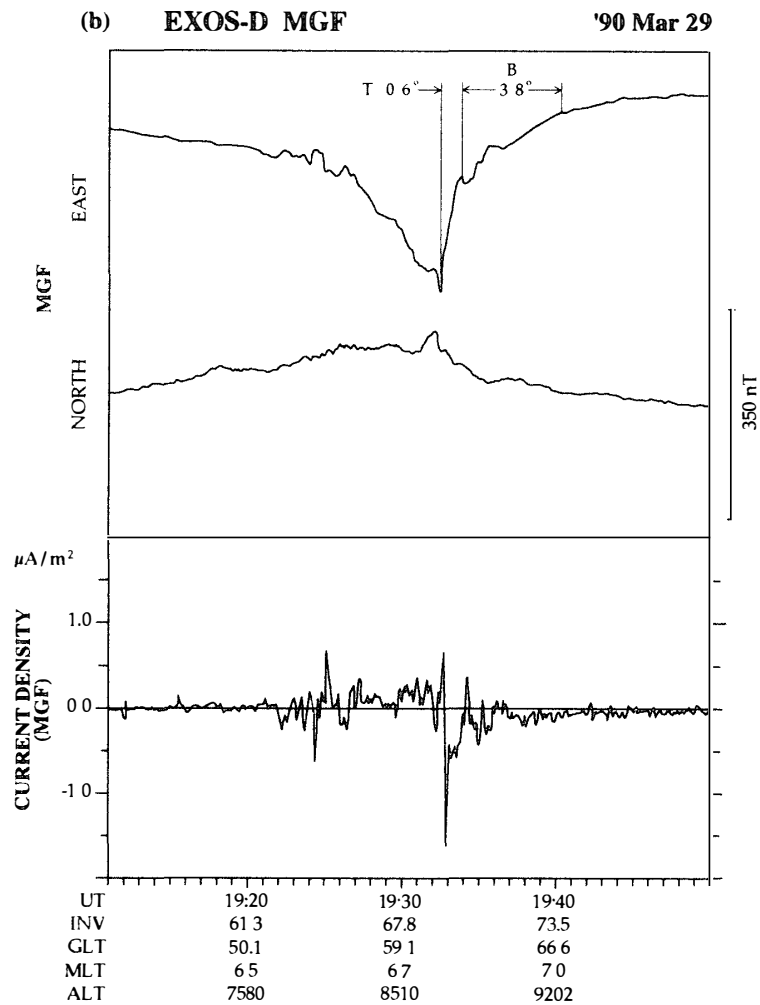
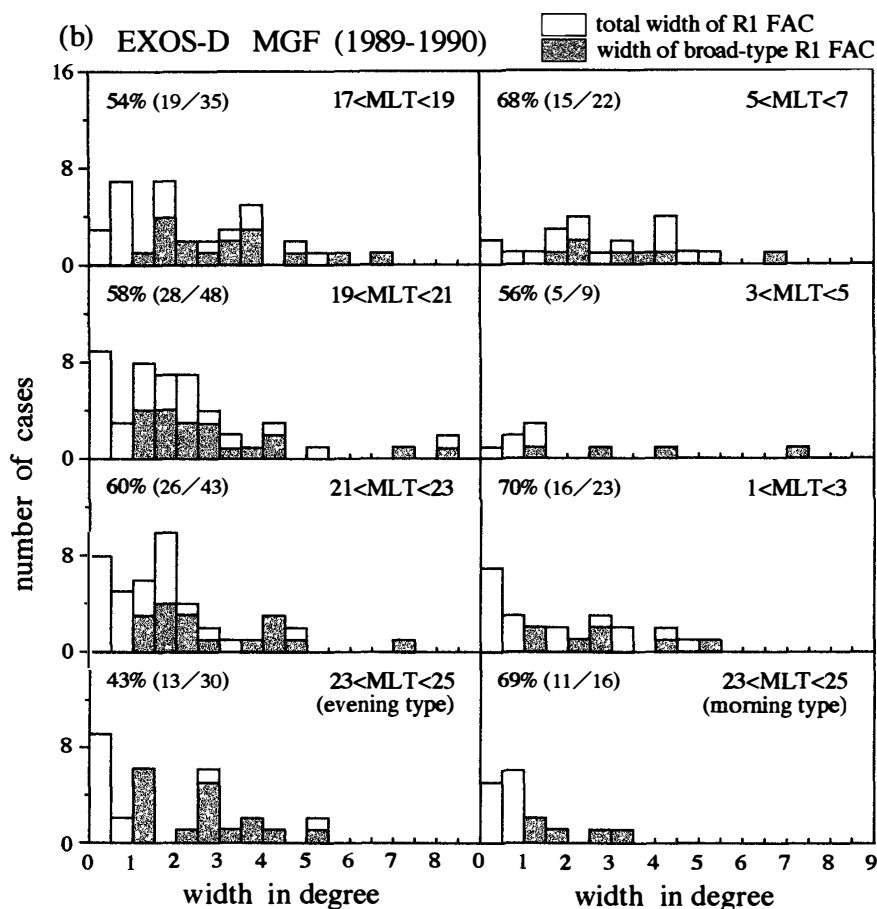
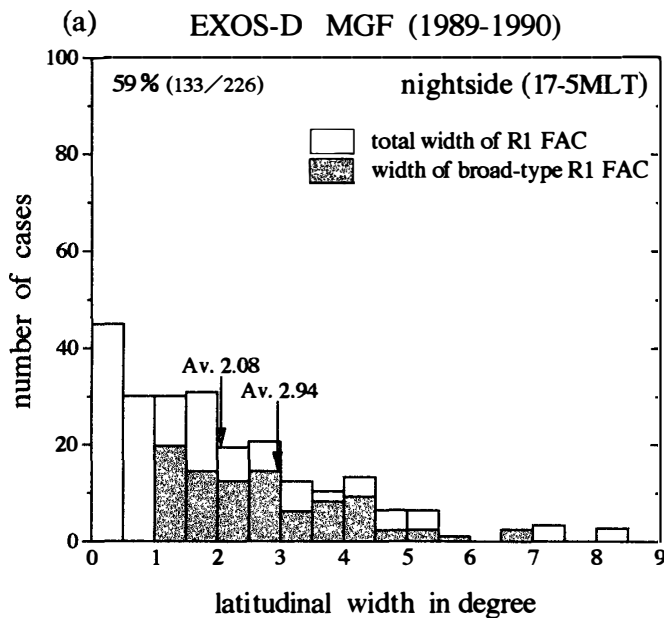


Fig. 6 (continued).

broad-type region 1 systems (without a T-structure) plotted against the latitudinal width. The average width of the broad-type region 1 current system is about  $2.9^\circ$ , while the averaged total width of the region 1 system is about  $2.1^\circ$ , which is consistent with the previous observations (e.g., IJIMA and POTEMRA, 1978). The number of the region 1 systems including the T-structure (corresponding to unshaded part of the histogram) is about 59% of the whole number of the identified region 1 systems. Figure 7b shows similar histograms for each two-hour MLT sector. In the 23–25 (= 01) MLT sector, two separate histograms are given for the evening-type (i.e., upward current) and morning-type (i.e., downward current) region 1 systems. The percentage of the number of the region 1 systems including the T-structure, relative to the whole number of the region 1 systems, in each MLT sector, is indicated. It is then found that over all the nighttime sectors, about 50 to 70% of the region 1 systems have the T-structure, although the number of morningside region 1 systems examined here is limited. The width distributions of the T-structure are shown for all MLT in Fig. 8a, and for each MLT sector in Fig. 8b. The average width of the T-structure is found to be about  $0.5^\circ$ . In summary, from the EXOS-D MGF data we find that the nightside region 1 FAC system often includes the thin current sheet (T-structure) of  $\sim 0.5^\circ$  in

Fig. 7. (a) Numbers of the region 1 FAC systems in the 17–5 MLT range versus the (total) latitudinal width of the system. The gray-shaded histogram shows the numbers of the broad-type region 1 FAC systems (without a T-structure) versus the system width. (b) Same as (a), but for each two-hour MLT sector. Two separate histograms in the 23–25 (=01) MLT sector are shown for the evening and morning types of the region 1 current system. In the upper left corner of each histogram in (a) and (b), the percentage of the number of the T-structures relative to the whole number of the region 1 systems is indicated together with these two numbers in a fraction.



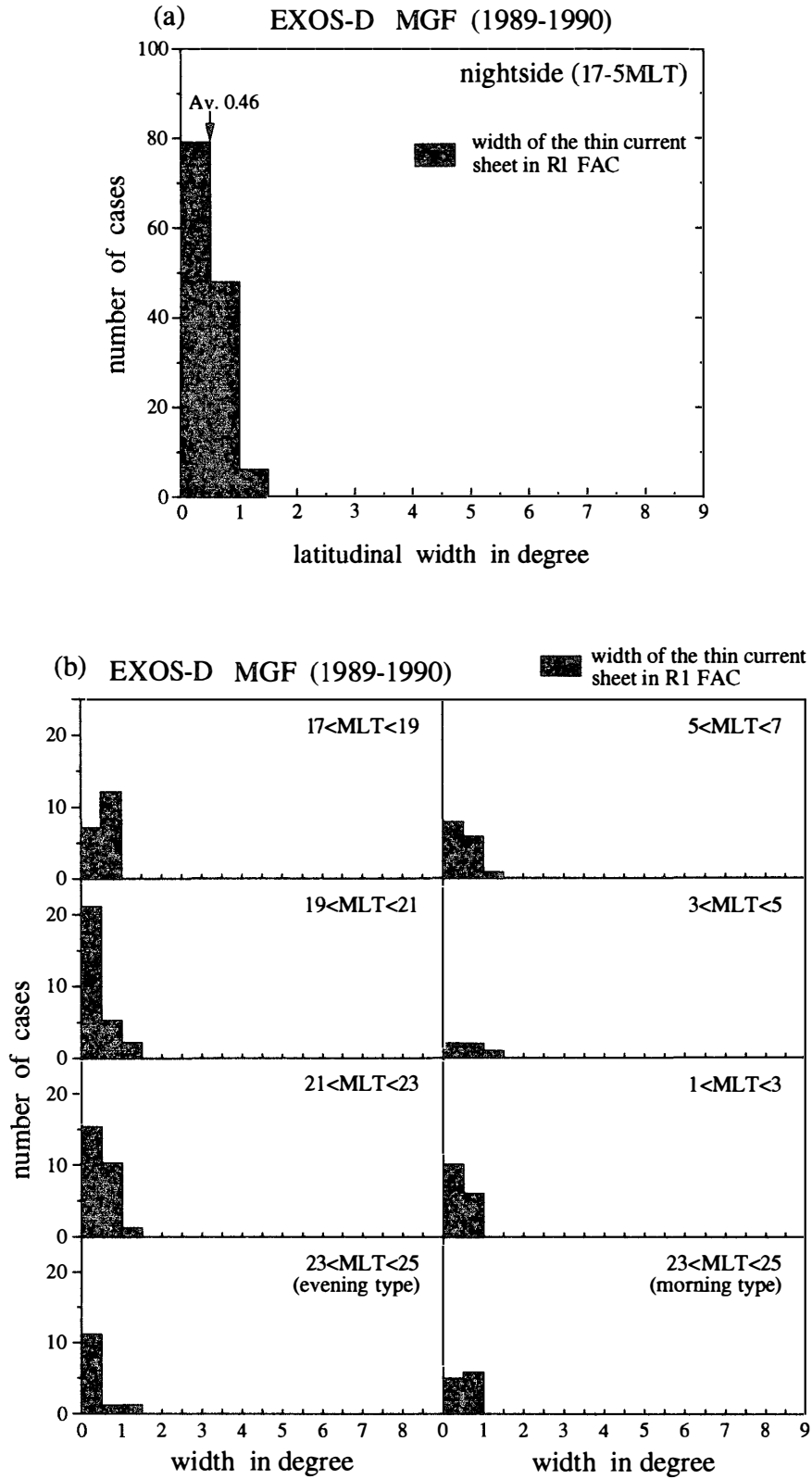


Fig. 8. (a) Numbers of the thin current sheets (*T*-structures) in the region 1 FAC systems in the 17-5 MLT range, versus the width of *T*-structure. (b) Same as (a), but for each two-hour MLT sector.

width, as a significant contributor to the total region 1 current intensity. (A possible formation mechanism of the T-structure is discussed by YAMAMOTO *et al.* (1999). In short, particle energization just inside the open/close boundary distorted by the plasma convection may be responsible for the formation of the T-structure.)

#### 4. Conclusions

Using the magnetic field data from the EXOS-D satellite, we have found that about 60% of the nightside region 1 field-aligned current systems have the latitudinal structure (T-structure) of a thin (on average,  $0.5^\circ$ ) current sheet with current intensity greater than one third of the total current intensity of the region 1 system. Sometimes the region 1 FAC is concentrated to a narrow region of  $\sim 0.5^\circ$  in width, namely most of its total current intensity is produced in that region. In the 20–04 MLT sector, when both of the T-structure and the boundary FAC system are simultaneously identified, the former is located just equatorward of the latter while they may partly overlap each other.

#### Acknowledgments

The authors are grateful to Prof. H. FUKUNISHI, Dr. T. NAGATSUMA and Dr. T. SAKANOI for providing us with the EXOS-D MGF data. The work of T. YAMAMOTO was supported in part by the joint research programs of Radio Atmospheric Science Center, Kyoto University, Uji, Kyoto, the Institute of Space and Astronautical Science, Sagamihara, Kanagawa, and the National Institute of Polar Research, Itabashi, Tokyo.

#### References

- BYTHROW, P.F., POTEIRA, T.A., ZANETTI, L.J., ERLANDSON, R.E., HARDY, D.A., RICH, F.J. and ACUNA, M. H. (1987): High latitude currents in the 0600 to 0900 MLT sector: observations from Viking and DMSP-F7. *Geophys. Res. Lett.*, **14**, 423–426.
- CRAVEN, J.D., KAMIDE, Y., FRANK, L.A., AKASOFU, S.-I. and SUGIURA, M. (1983): Distribution of aurora and ionospheric currents observed simultaneously on a global scale. *Magnetospheric Currents*, ed. by T.A. POTEIRA. Washington, D.C., Am. Geophys. Union, 137–146 (*Geophys. Monogr. Ser.*, Vol. 28).
- FUJII, R., HOFFMAN, R.A., ANDERSON, P.C., CRAVEN, J.D., SUGIURA, M., FRANK, L.A. and MAYNARD, N.C. (1994): Electrodynamics parameters in the nighttime sector during auroral substorms. *J. Geophys. Res.*, **99**, 6093–6112.
- FUKUNISHI, H., FUJII, R., KOKUBUN, S., TOHYAMA, F., MUKAI, T. and OYA, H. (1991): Small-scale field-aligned currents observed by the AKEBONO (EXOS-D) satellite. *Geophys. Res. Lett.*, **18**, 297–300.
- FUKUNISHI, H., TAKAHASHI, Y., NAGATSUMA, T., MUKAI, T. and MACHIDA, S. (1993): Latitudinal structures of nightside field-aligned currents and their relationships to the plasma sheet regions. *J. Geophys. Res.*, **98**, 11235–11255.
- HAERENDEL, G., FREY, H.U., BAUER, O.H., RIEGER, E., CLEMMONS, J., BOEHM, M. H., WALLIS, D.D. and LÜHR, H. (1994): Inverted-V events simultaneously observed with the Freja satellite and from the ground. *Geophys. Res. Lett.*, **21**, 1891–1894.
- HAREL, M., WOLF, R.A., SPIRO, R.W., REIFF, P.H., CHEN, C.-K., BURKE, W.J., RICH, F.J. and SMIDDY, M. (1981): Quantitative simulation of a magnetospheric substorm, 2, Comparison with observations. *J.*

- Geophys. Res., **86**, 2242–2260.
- HEINEMANN, N.C., GUSSENHOVEN, M.S., HARDY, D.A., RICH, F.J. and YEH, H.-C. (1989): Electron/ion precipitation differences in relation to region 2 field-aligned currents. *J. Geophys. Res.*, **94**, 13593–13600.
- IJIMA, T. and POTEIRA, T.A. (1976a): The amplitude distribution of field-aligned currents at northern high latitudes observed by TRIAD. *J. Geophys. Res.*, **81**, 2165–2174.
- IJIMA, T. and POTEIRA, T.A. (1976b): Field-aligned currents in the dayside cusp observed by TRIAD. *J. Geophys. Res.*, **81**, 5971–5979.
- IJIMA, T. and POTEIRA, T.A. (1978): Large-scale characteristics of field-aligned currents associated with substorms. *J. Geophys. Res.*, **83**, 599–615.
- LYONS, L.R. and SPEISER, T.W. (1982): Evidence for current sheet acceleration in the geomagnetic tail. *J. Geophys. Res.*, **87**, 2276–2286.
- NAGATSUMA, T., FUKUNISHI, H. and MUKAI, T. (1995): Spatial relationships between field-aligned currents and suprathermal electron beams observed at the poleward boundary of the nightside auroral oval. *J. Geophys. Res.*, **100**, 1625–1637.
- POTEIRA, T.A., ZANETTI, L.J., ERLANDSON, R.E., BYTHROW, P.F., GUSTAFSSON, G., ACUNA, M.H. and LUNDIN, R. (1987): Observations of large-scale Birkeland currents with Viking. *Geophys. Res. Lett.*, **14**, 419–422.
- SOUTHWOOD, D.J. (1977). The role of hot plasma in magnetospheric convection. *J. Geophys. Res.*, **82**, 5512–5520.
- STASIEWICZ, K. and POTEIRA, T. (1998): Multiscale current structures observed by Freja. *J. Geophys. Res.*, **103**, 4315–4325.
- TSYGANENKO, N.A. (1989): A magnetospheric magnetic field model with a warped tail current sheet. *Planet. Space Sci.*, **37**, 5–20.
- VASYLIUNAS, V.M. (1970): Mathematical models of magnetospheric convection and its coupling to the ionosphere. *Particles and Fields in the Magnetosphere*, ed. by B.M. MCCORMAC. Norwell, D. Reidel, 60–71.
- WOLF, R.A. (1983): The quasi-static (slow-flow) region of the magnetosphere. *Solar-Terrestrial Physics*, ed. by R.L. CAROVILLANO and J.M. FORBES. Norwell, D. Reidel, 303–368.
- YAMAMOTO, T. and INOUE, S. (1998): Quasi-steady production of region 1 and region 2 field-aligned currents. *Proc. NIPR Symp. Upper Atmos. Phys.*, **11**, 106–120.
- YAMAMOTO, T., INOUE, S., NISHITANI, N., OZAKI, M. and MENG, C.-I. (1996): A theory for generation of the paired region 1 and region 2 currents. *J. Geophys. Res.*, **101**, 27199–27222.
- YAMAMOTO, T., INOUE, S. and MENG, C.-I. (1997a): Numerical study on dynamics and polarization of the hot plasma torus in the magnetosphere: Cause of generation of the paired region 1 and region 2 field-aligned currents. *J. Geomagn. Geoelectr.*, **49**, 879–922.
- YAMAMOTO, T., INOUE, S. and MENG, C.-I. (1997b): Effect of anomalous cross-field diffusion on the field-aligned current generation. *J. Geomagn. Geoelectr.*, **49**, 923–945.
- YAMAMOTO, T., INOUE, S., OZAKI, M. and NISHITANI, N. (1999): Distortion of the outer boundary of the closed region in the Tsyganenko magnetic field model. *Adv. Polar Upper Atmos. Res.*, **13**, 89–104.
- YAMAUCHI, M., LUNDIN, R., ELIASSON, L., OHTANI, S. and CLEMMONS, J.H. (1998): Relationship between large-, meso-, and small-scale field-aligned currents and their current carriers. *Polar Cap Boundary Phenomena*, ed. by J. MOEN *et al.* Dordrecht, Kluwer Academic Publ., 173–188 (NATO ASI series, series C, Vol. 509).
- YANG, Y.S., SPIRO, R.W. and WOLF, R.A. (1994): Generation of region 1 current by magnetospheric pressure gradients. *J. Geophys. Res.*, **99**, 223–234.

(Received February 3, 1999; Revised manuscript accepted April 28, 1999)